

lncRNAs as Novel Indicators of Patients' Prognosis in Stage I Epithelial Ovarian Cancer: A Retrospective and Multicentric Study

Paolo Martini¹, Lara Paracchini², Giulia Caratti², Maurizia Mello-Grand³, Robert Fruscio⁴, Luca Beltrame², Enrica Calura¹, Gabriele Sales¹, Antonella Ravaggi⁵, Eliana Bignotti⁵, Franco E. Odicino⁶, Enrico Sartori⁶, Patrizia Perego⁷, Dionyssios Katsaros⁸, Ilaria Craparotta², Giovanna Chiorino³, Stefano Cagnin^{1,9}, Laura Mannarino², Lorenzo Ceppi⁴, Costantino Mangioni¹⁰, Chiara Ghimenti³, Maurizio D'Incalci², Sergio Marchini², and Chiara Romualdi¹

Abstract

Purpose: Stage I epithelial ovarian cancer (EOC) represents about 10% of all EOCs and is characterized by good prognosis with fewer than 20% of patients relapsing. As it occurs less frequently than advanced-stage EOC, its molecular features have not been thoroughly investigated. We have demonstrated that in stage I EOC *miR-200c-3p* can predict patients' outcome. In the present study, we analyzed the expression of long non-coding RNAs (lncRNA) to enable potential definition of a non-coding transcriptional signature with prognostic relevance for stage I EOC.

Experimental Design: 202 snap-frozen stage I EOC tumor biopsies, 47 of which relapsed, were gathered together from three independent tumor tissue collections and subdivided into a training set ($n = 73$) and a validation set ($n = 129$). Median

follow up was 9 years. lncRNAs' expression profiles were correlated in univariate and multivariate analysis with overall survival (OS) and progression-free survival (PFS).

Results: The expression of *lnc-SERTAD2-3*, *lnc-SOX4-1*, *lnc-HRCT1-1*, and *PVT1* was associated in univariate and multivariate analyses with relapse and poor outcome in both training and validation sets ($P < 0.001$). Using the expression profiles of *PVT1*, *lnc-SERTAD2-3*, and *miR-200c-3p* simultaneously, it was possible to stratify patients into high and low risk. The OS for high- and low-risk individuals are 36 and 123 months, respectively (OR, 15.55; 95% confidence interval, 3.81–63.36).

Conclusions: We have identified a non-coding transcriptional signature predictor of survival and biomarker of relapse for stage I EOC. *Clin Cancer Res*; 23(9); 2356–66. ©2016 AACR.

Introduction

Patients diagnosed with stage I epithelial ovarian cancer (EOC) tend to have a good prognosis, with more than 80% surviving five

years from the diagnosis. This situation differs significantly from patients with the more commonly diagnosed EOCs of stage III/IV. Stage I EOC is a rare disease, which is diagnosed in less than 10% of EOC patients (1, 2). The clinical management of stage I EOC is confounded by the difficulty to identify at diagnosis, the small fraction of patients (almost 20%) who will not respond to platinum-based therapy and will relapse with progressively resistant and fatal disease (1, 3).

Tumor grade is currently the most common prognostic parameter for stage I disease. Routinely used histologic and clinical classifiers are unable to efficiently predict those patients who will eventually relapse and thus could immediately benefit from different therapeutic approaches. Thus, it is of utmost importance to identify molecular biomarkers able to predict the outcome of patients with stage I EOC and/or to stratify such patients' risk of relapse (4).

We have recently identified genetic and epigenetic defects in the control of transcriptional regulation which correlate with prognosis of stage I EOC (5–7). Specifically, we have shown that *miR-200c-3p* is a predictor of survival and a biomarker of relapse in stage I EOC, independent of clinical covariates (6). Further analysis based on integration of miRNAs and gene-expression signatures, defined that *miR-200c-3p* is an element of an integrated signature classifier (ISC) based on 16 miRNAs and 10 coding genes that control cell-cycle progression, Activin/Inhibin pathways and Hedgehog signaling (5). The expression levels of the ISC

¹Department of Biology, University of Padova, Padova, Italy. ²Department of Oncology, IRCCS-Istituto di Ricerche Farmacologiche "Mario Negri", Milano, Italy. ³Cancer Genomics Laboratory, Edo and Elvo Tempia Valenta Foundation, Biella, Italy. ⁴Clinic of Obstetrics and Gynaecology, University of Milano-Bicocca, San Gerardo Hospital, Monza, Italy. ⁵Division of Gynaecologic Oncology, "Angelo Nocivelli" Institute of Molecular Medicine, University of Brescia, Brescia, Italy. ⁶Department of Obstetrics and Gynecology, University of Brescia, Brescia, Italy. ⁷Pathology Unit University of Milan-Bicocca, San Gerardo Hospital, Monza, Italy. ⁸Azienda Ospedaliero-Universitaria Città della Salute, Presidio S Anna e Department of Surgical Science, Gynecology, University of Torino, Torino, Italy. ⁹C.R.I.B.I. Biotechnology Centre, University of Padova, Padova, Italy. ¹⁰P.O.A Manzoni, Lecco, Italy.

Note: Supplementary data for this article are available at Clinical Cancer Research Online (<http://clincancerres.aacrjournals.org/>).

P. Martini and L. Paracchini contributed equally to this article.

S. Marchini and C. Romualdi share last authorship.

Corresponding Author: Maurizio D'Incalci, IRCCS - Istituto di Ricerche Farmacologiche "Mario Negri," Via La Masa 19, Milano 20156, Italy. Phone/Fax: 39.0239014.571/734; E-mail: maurizio.dincalci@marionegri.it

doi: 10.1158/1078-0432.CCR-16-1402

©2016 American Association for Cancer Research.

Translational Relevance

The present study shows that in stage I epithelial ovarian cancer, defects in lncRNA transcription regulation of *lnc-SER-TAD2-3*, *lnc-SOX4-1*, *lnc-HRCT1-1*, and *PVT1* are independent prognostic markers of relapse and poor prognosis. These findings corroborate the idea that the expression levels of the transcripts can be used to stratify stage I ovarian cancer patients more accurately, thus selecting the most appropriate therapies according to their risk of relapse. In addition, the findings provide the rationale to investigate novel therapies in the selected stage I ovarian cancer patients' cohorts.

stratified patients' risk of relapse into high and low risk better than conventional clinical- and histologic-based classifiers (5).

To allow dissection of detailed mechanisms of transcriptional regulation associated with poor prognosis and relapse in stage I EOC, we focused our attention on another type of non-coding RNAs with regulatory functions: the long non-coding RNAs (lncRNA). lncRNAs are broadly classified as transcripts longer than 200 nucleotides without coding potential but with essential biological properties. lncRNA genes are evolutionarily conserved and often expressed in a tissue-specific manner (8). Although their functions have been poorly characterized to date, evidence suggests that lncRNAs contribute to the dynamic regulation of gene-expression programs by several mechanisms (9–12). lncRNA expression patterns correlated with various cellular processes (13), and deregulation of lncRNA expression emerges as an important determinant of tumor development, progression, and therapy response (10, 14, 15). Therefore, the elucidation of the roles of lncRNAs in tumors might allow deeper insights into the molecular biology of cancer and improve response to therapy.

The aim of this work was to correlate for the first time the clinical outcome of patients with EOC stage I with expression of lncRNAs. Correlations of this kind might help reveal biological mechanisms that determine the response of patients with stage I EOC to platinum-based chemotherapy, and they might suggest novel therapeutic strategies for stage I EOC.

Material and Methods

Tissue sample collection and experimental design

A cohort of 202 snap-frozen tumor biopsies was collected from three independent Italian tumor tissue collections, as previously described (5, 16). Written informed consent was obtained from all patients enrolled in the study according to the Declaration of Helsinki principles. Patient information pertaining to anatomy and pathology was registered, and follow-up data were obtained from regular gynecological and oncological check-ups. The ethical committees of the centers taking part in the study approved the collection and the use of the samples. A detailed description of the three cohorts is described in Table 1 and Supplementary Section S1. Concerning the experimental design, patients were randomly split into a 73-patient training set and a 129-patient validation set. In the random selection histotype and grade annotations were taken into account to achieve a homogeneous distribution of these variables in both datasets. Except for endometrioid histotype (test of proportion $P = 0.0276$), all the other categories were equally distributed. The sample size in the training set was

estimated with the powerSurvEpi ver. 0.0.9 – CRAN R package. We wanted the sample size to be the minimal one required to allow a statistical power greater than 0.8 to detect a statistically significant hazard ratio (HR) greater than 1.6 (with alpha level set to 0.05) using a Cox proportional hazard model. The present study was carried out following the REMARK guidelines (ref. 17; see Supplementary Section S1 and Supplementary Table S1.1).

lncRNA expression profile data analysis and signature validation

lncRNA and gene-expression profiles were established according to well-standardized protocols (6, 16). Details are reported in Supplementary Section S2. The raw data are available at Array Express E-MTAB-1814. lncRNA expression levels were validated by RT-qPCR as previously described (detailed in Supplementary Section S2 and references; refs. 6, 16). miR-200c-3p expression levels were measured with commercial available reagents (Qiagen) following protocols previously described (6).

lncRNA subcellular localization

lncRNAs subcellular localization enrichment was measured by microarray and RT-qPCR analyses in nuclear and cytoplasmic extracts from 5 well-known ovarian cancer cell lines (OVCAR8, OVCAR3, A2780, OVCA432, and CAOV3). Microarray and RT-qPCR experiments were performed as described for lncRNAs and mRNA expression profiles (for details see Supplementary Section S3). The five ovarian cancer cell lines (OVCAR8, OVCAR3, A2780, OVCA432, and CAOV3) were tested and authenticated before their ultimate storage (October 2014) in cell growth medium supplemented with an equal volume of FBS and a double volume of "cryoprotective medium" (Lonza). Cells were stored in liquid nitrogen.

Network and pathway analysis

lncRNA-target co-expression was identified using a network reconstruction approach called ARACNE (upgraded with Package parmigene ver. 1.0.2 for R-language; ref. 18). Briefly, we computed the mutual information (MI) between all mRNAs, lncRNAs and miRNAs. Significant interactions (MI \geq 99th percentile of a null distribution obtained by permutations of the dataset) were identified through the ARACNE algorithm. The co-expression network was used to derive co-expressed interactors with the lncRNAs. A hypergeometric test was used to select those pathways showing a significant enrichment in lncRNA co-expressed interactors (see Supplementary Section S4).

For each lncRNA, we performed pathway analysis using the microGraphite pipeline (19–21) comparing the expression profiles of patients with good and bad prognoses according to the selected lncRNA expression profile (median value as threshold—see Supplementary Section S4).

Statistical analysis

All statistical analyses were carried out in R language environment (R ver. 3.3.1) unless otherwise stated. Sam-paired T test was performed using TMEV (www.tm4.org - ver. 4.8). Univariate and multivariate survival analyses were performed using respectively Kaplan–Meier (KM) curves with log-rank test and the Cox model with grade, histotype and chemotherapy as covariates. Expression values were converted into classes High and Low for values above and below the median, respectively. The Wilcoxon test

Martini et al.

Table 1. Clinical and histologic annotations

Clinical	Type	Training N (%)	Validation N (%)	OS - CI	OS P value	PFS - CI	PFS P value
Histotypes	Clear cell	16 (21.9%)	21 (16.3%)	—	—	—	—
	Endometrioid	19 (26.0%)	55 (42.6%)	0.48 (0.19–1.25)	0.1336	0.8 (0.34–1.9)	0.6202
	Mucinous	15 (20.5%)	20 (15.5%)	0.82 (0.31–2.14)	0.6852	0.44 (0.14–1.36)	0.1555
	Serous high grade	16 (21.9%)	26 (20.2%)	0.86 (0.34–2.19)	0.7553	1.33 (0.57–3.12)	0.5086
	Serous low grade	7 (9.6%)	7 (5.4%)	0.2 (0.03–1.62)	0.1329	0.62 (0.16–2.34)	0.4785
Grades	G1	17 (23.3%)	38 (29.5%)	—	—	—	—
	G2	23 (31.5%)	40 (31.0%)	0.86 (0.33–2.23)	0.7533	1.04 (0.44–2.44)	0.9348
	G3	33 (45.2%)	51 (39.5%)	1.91 (0.87–4.2)	0.109	2.21 (1.06–4.6)	0.0333
Type	I	53 (72.6%)	88 (68.2%)	—	—	—	—
	II	20 (27.4%)	41 (31.8%)	1.09 (0.55–2.18)	0.801	1.66 (0.93–2.96)	0.087
FIGO substage	a	23 (31.5%)	46 (35.7%)	—	—	—	—
	b	4 (5.5%)	11 (8.5%)	1.7 (0.47–6.21)	0.42	1.52 (0.42–5.46)	0.5226
	c	46 (63.0%)	72 (55.8%)	1.69 (0.81–3.55)	0.1634	2.11 (1.07–4.19)	0.0321
Chemotherapy	no	16 (21.9%)	27 (20.9%)	—	—	—	—
	yes	41 (56.2%)	95 (73.6%)	0.98 (0.45–2.15)	0.9619	2.99 (1.17–7.65)	0.0225
	missing	16 (21.9%)	7 (5.4%)	—	—	—	—
Mean Age [min-max] years		62 [30–87]	61 [25–88]	1.02 (1–1.05)	0.0769	1.01 (0.99–1.04)	0.3231
Relapsing	N	52 (71.2%)	101 (78.3%)	—	—	—	—
	Y	21 (28.8%)	26 (20.2%)	—	—	—	—
	NA	0 (0)	2 (1.5%)	—	—	—	—
Vital status at the last follow-up	AWD	2 (2.7%)	4 (3.1%)	—	—	—	—
	DOC	2 (2.7%)	5 (3.9%)	—	—	—	—
	DOD	15 (20.5%)	15 (11.6%)	—	—	—	—
	NED	54 (74.0%)	101 (78.3%)	—	—	—	—
	UNK	0 (0)	4 (3.1%)	—	—	—	—
Mean follow-up [min-max] years		9 (1–18)	6 (0–18)	—	—	—	—
Total number of patients		73	129	—	—	—	—

NOTE: Table summarizes the main clinical and histopathologic features of 202 patients enrolled in the study and their correlation in univariate model with OS and PFS. Patients were randomized into a training set ($n = 73$) and a validation set ($n = 129$). G1 = Grade 1, G2 = Grade 2, G3 = Grade 3, AWD = Awaiting Decision, DOC = Dead of Other Cause, DOD = Dead of EOC, FIGO = Federation Internationale des Gynaecologues et Obstetristes; NED = No Evidence of Disease.

(two-sided) was used to compare median expression levels of relapsers versus non-relapsers. A hypergeometric test (phyper R function) was used to compute the enrichment of first neighbors of lncRNAs in KEGG pathways. Test for equal proportion was carried out using `pro.test` R function.

Results

Patient characteristics

Table 1 shows the histopathology of the tumor samples and the number of patients who received post-surgical chemotherapy. All biopsies were from patients naïve to chemotherapy at the time of primary surgery. Histopathologic features have been investigated, by independent pathologists according to FIGO guidelines (22). Subtypes and grades were evenly distributed across patients, that is, they occurred in equal proportions between the training set ($n = 73$) and the validation set ($n = 129$) as described under Materials and Methods. The mean follow-up time was 9 years (1–18 years) for the training set and 6 years (0–18 years) for the validation set. At the last follow-up 76.7% of patients were still alive ($n = 54$, 74.0% of patients in the training set and $n = 101$, 78.3% of patients in the validation set), and 76.7% were progression free ($n = 52$, 71.2% of patients in the training set and $n = 101$, 78.3% of patients in the validation set). As to the chemotherapy regimens used, 56.2% of patients ($n = 41$) in the training set and 73.6% of patients ($n = 95$) in the validation set received platinum-based adjuvant chemotherapy (overall 67.3%, $n = 136$). Twenty-one of the 73 samples in the training set (28.8%) and 26 of the 129 samples in the validation set

(20.2%) originated from patients who relapsed after platinum-based chemotherapy. These are referred to in the following as relapsers (overall, 23.3%, $n = 47$). The Univariate Cox proportional hazards model (Table 1) indicates that grade "G3," substage "c" and chemotherapy were significantly associated with progression-free survival (PFS). No association was observed for overall survival (OS). As detailed in Supplementary Section S1 and as published previously (16), survival models show that this cohort is representative of stage I EOC, as PFS and OS are similar to those reported in the literature with respect to substage, grading, and histotype (23).

Overall study design

We developed a multidisciplinary approach summarized in Supplementary Section S1 (Supplementary Fig. S1.1) Briefly, in the training set we screened more than 5000 lncRNAs for association with OS and PFS using microarray-based expression levels. Orthogonal multivariate analysis of both training and validation sets by RT-qPCR identified four lncRNAs the expression levels of which were associated with OS and PFS independent of clinical covariates. To obtain deeper insights of biological functions of selected lncRNAs, *in vitro* ovarian cancer cell lines were used as a model to investigate subcellular localization. Three out of four lncRNAs with prognostic relevance were clearly localized in the nuclei allowing prediction of their roles in transcriptional regulation. On the basis of this assumption and using microGraphite pipeline (19), we derived a subnet of a biological network (defined from now onwards as regulatory circuit) with prognostic relevance, tightly associated with the lncRNAs expression. To

conclude, we combined the expression signatures of both lncRNAs and miRNAs.

Identification of lncRNAs associated with clinical parameters

lncRNAs expression profiles were obtained by microarray experiments on the training set (Supplementary Section S2). To identify lncRNAs with potential prognostic value for stage I EOC, we searched for lncRNAs related to disease progression. To that end the univariate survival model was used to individually test all 5,156 lncRNA probes for their association with OS and PFS. This strategy resulted in 67 lncRNA probes (corresponding to 63 different lncRNAs) that correlated significantly with patients' survival, either in terms of OS or PFS. Using grades and histotypes as covariates, we evaluated the effects of lncRNA expression levels on PFS or OS. Multivariate Cox proportional hazards model selected 26 out of the 67 probes (corresponding to 25 lncRNA genes) the expression levels of which correlated significantly with either OS or PFS (Supplementary Section S2 and Supplementary Table S2.2).

Because the above analyses were based on array probe measures obtained within a complex mixture of transcripts, orthogonal validation of lncRNAs' expression by RT-qPCR was performed to confirm their clinical relevance. To correct for a potential batch effect, RNA for RT-qPCR experiments was purified from a second aliquot of snap frozen material from the same patients selected for the training set. We were able to design primer pairs for only 10 out of 25 selected lncRNAs (see Supplementary Section S2 and Supplementary Table S2.1), as the necessity to test for specific isoforms of lncRNAs constituted a considerable challenge in the design of primers compatible with RT-qPCR parameters.

Influence of lncRNAs expression on survival in the training set

RT-qPCR data obtained in the training set were used to (i) investigate the potential correlation of selected lncRNAs with clinical variables and (ii) stratify, at diagnosis, patients for risk of relapse.

Table 2 shows that the expression levels of four lncRNAs, namely *lnc-SERTAD2-3*, *lnc-SOX4-1*, *lnc-HRCT1-1*, and *lnc-MYC-2* (also known as *PVT1*) were associated in both univariate and multivariate analyses with OS and PFS ($P < 0.05$). Univariate model analysis suggests that patients with low expression levels of *lnc-SERTAD2-3*, *lnc-SOX4-1*, *lnc-HRCT1-1*, and *PVT1* had longer survival and longer PFS than those with high levels.

Figure 1A shows survival plots for the prognostic groups identified by these four lncRNAs. KM curves plotting OS or PFS against median expression values of each of the four selected lncRNAs confirmed these inferences. For example, patients with high levels of *lnc-SERTAD2-3* had shorter OS and PFS than those with low levels. The respective OS medians were 35 months versus 138 months with odds-ratio (OR), 9.32; 95% confidence interval (CI), 1.91–45.32. The respective PFS medians were 45 months versus 135 months with OR, 14.76; 95% CI, 3.07–70.97. KM plots for lncRNAs that did not show such correlations, and median PFS and OS values for each lncRNA, are shown in Supplementary Section 2 (Supplementary Fig. S2.2 and Supplementary Table S2.3, respectively).

lncRNA expression signature and survival in term of OS/PFS including clinical features (histotypes, grades, and chemotherapy) were subjected to multivariate analysis using the Cox proportional hazards model. Expression levels of *lnc-SERTAD2-3*, *lnc-SOX4-1*, *lnc-HRCT1-1*, and *PVT1* are independent prognostic

markers of survival (Table 2). *lnc-ABCB4-1* variant 1 was associated only with PFS ($P = 0.048$ and $P = 0.3$ for PFS and OS, respectively) in multivariate analysis. It was therefore excluded from downstream analysis (Table 2). No association was observed for any of the other lncRNAs analyzed.

As for potential stratification for risk of relapse (point ii), the median distribution levels of normalized fluorescence intensity and the interquartile range (IQR) of each lncRNA in relapsers ($n = 21$) were compared with non-relapsers ($n = 52$). Analysis by Wilcoxon test shows significant differences in the expression level between relapsers and non-relapsers for five of the ten selected lncRNAs (Table 2). Both variants of *lnc-ABCB4-1* were underexpressed in relapsers compared with non-relapsers, while *lnc-SERTAD2-3*, *lnc-SOX4-1*, *lnc-HRCT1-1*, and *PVT1* were overexpressed in relapsers.

In conclusion, the results suggest a lncRNA-based prognostic signature for stage I EOC whose expression stratifies patient risk of relapse and is an independent prognostic marker of poor outcome.

lncRNA signature analysis in the validation set

To demonstrate the reproducibility and the robustness of the identified lncRNA-based prognostic signature, we validated our results in an independent set of patients.

Data reported in Table 2 confirms that the expression levels of *lnc-SERTAD2-3*, *lnc-SOX4-1*, *lnc-HRCT1-1*, and *PVT1* affect survival also in this set of patients.

Analysis by univariate model suggests that patients with high expression levels of these four lncRNAs had a shorter survival both in terms of OS and PFS than those with low expression levels. Figure 1B shows the KM curves and results of the log-rank test for the four lncRNAs both for OS (*lnc-SERTAD-2* P value = 0.00776; *lnc-SOX4-1* P value = 0.0577; *lnc-HRCT1-1* P value = 0.000587; *PVT1* P value = 0.000108) and PFS (*lnc-SERTAD-2* P value = 0.000429; *lnc-SOX4-1* P value = 0.0197; *lnc-HRCT1-1* P value = $5.92e-06$; *PVT1* P value = $2.67e-07$). For each lncRNA, the complete median values for PFS and OS with relative OR and CI are shown in Supplementary Table S2.4 (Supplementary Section S2).

Analysis by the Cox proportional hazard model revealed that *lnc-SERTAD2-3*, *lnc-SOX4-1*, *lnc-HRCT1-1*, and *PVT1* are significant prognostic factors for OS and PFS even when corrected for grade, histotypes and chemotherapy (Table 2).

Comparing the median expression value of selected lncRNAs between relapsers ($n = 26$) and non relapsers ($n = 101$), we observed that *lnc-SERTAD2-3*, *lnc-SOX4-1*, *lnc-HRCT1-1*, and *PVT1* were significantly over-expressed in tumor biopsies of the relapsers compared with non relapsers (Table 2). Stage I EOC is not one single disease and patient characteristics differ in terms of histotype. Therefore, we questioned whether the prognostic value of selected lncRNA signatures is maintained across different histotypes (Table 3). Multivariate analysis performed on the entire cohort of patients ($n = 202$) suggests that the predictive value of *lnc-SERTAD2-3*, *lnc-SOX4-1*, *lnc-HRCT1-1*, and *PVT1* is independent of histologic covariates (Table 3).

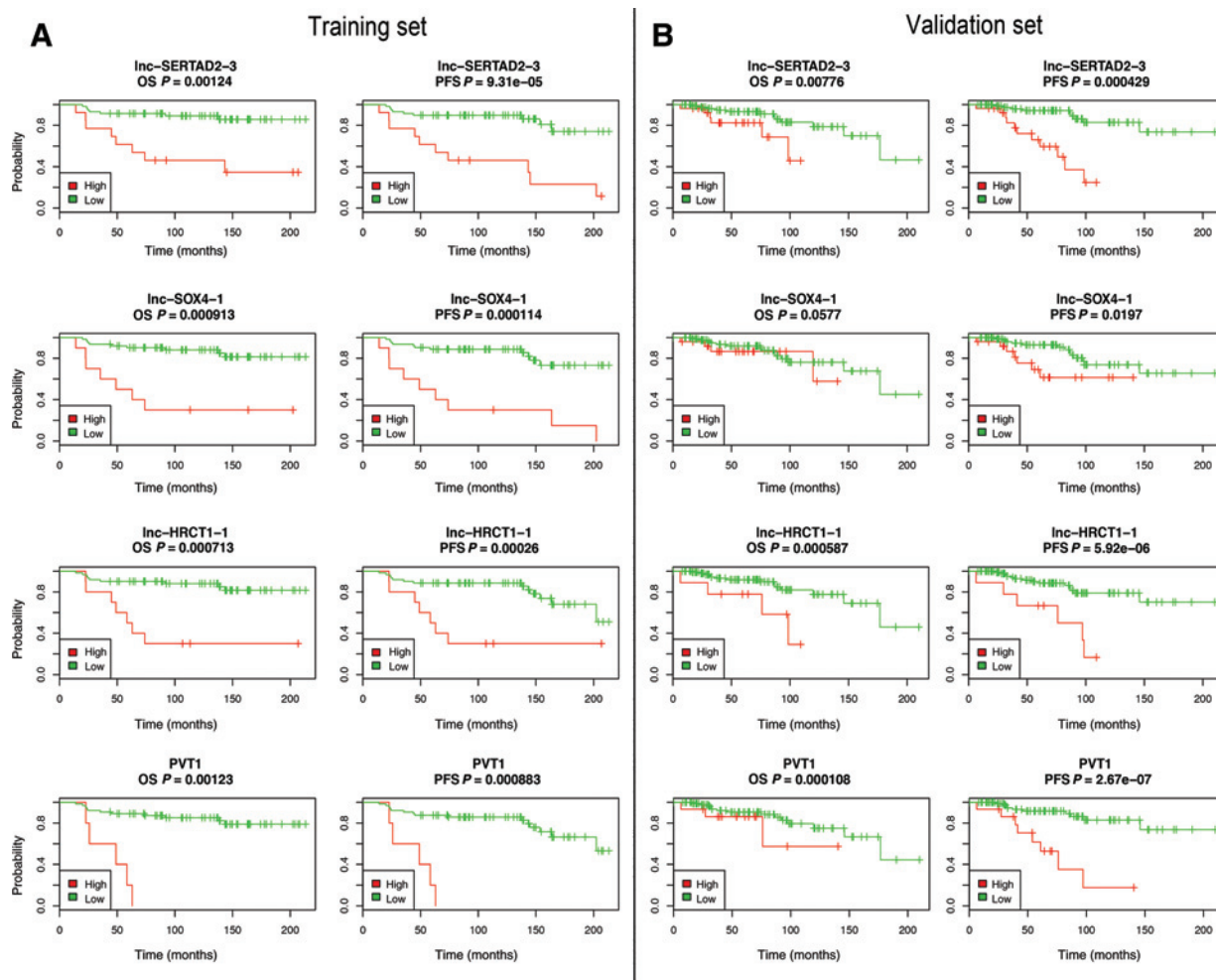
Subcellular localization of lncRNA

Understanding how lncRNAs give rise to specific patterns of gene expression requires the knowledge of their cellular localization. Although the knowledge of the mechanisms of action of

Table 2. Correlation of lncRNA expression to OS and PFS

	OS			PFS			Relapsers versus nonrelapsers			
	Univariate analysis		Multivariate analysis	Univariate analysis		Multivariate analysis	Relapsers		Nonrelapsers	
	P	HR high vs. low (95% CI)	P ^a	P	HR high vs. low (95% CI)	P ^a	Median (IQR)	Median (IQR)	Ratio	P ^b
Training set										
<i>lnc-VSTM2B-9</i>	0.57	1.3 (1-1.8)	0.07	0.77	1.3 (1.0-1.7)	0.05	66.3 (50.1-148.4)	56.4 (28.4-163.4)	4.1	0.80
<i>lnc-SERTAD2-3</i>	1.24e-03	2.0 (1.3-3.1)	0.0014	9.31e-05	1.9 (1.3-2.6)	4e-04	150.1 (63.5-365.4)	18.6 (3.3-58.9)	10.3	1.21e-07
<i>lnc-SOX4-1</i>	9.13e-04	1.8 (1.3-2.4)	4e-04	1.14e-04	1.6 (1.3-2.1)	2e-04	287.3 (159.9-795.2)	57.3 (19.6-114.7)	11.3	1.73e-07
<i>lnc-ST3GAL1-1</i>	0.58	1.1 (0.9-1.4)	0.19	0.91	1.1 (0.9-1.4)	0.16	15.1 (3.6-85.2)	15.3 (4.0-60.1)	2.1	0.89
<i>lnc-HRCT1-1</i>	7.13e-04	1.5 (1.2-1.9)	2e-04	2.6e-04	1.54 (1.3-1.9)	2.1e-05	96.4 (56.3-258.9)	15.7 (4.1-58.9)	12.1	3.41e-07
<i>lnc-PHF15-2</i>	0.80	1.1 (0.8-1.4)	0.57	0.85	1.1 (0.9-1.3)	0.29	16.9 (2.0-76.0)	19.9 (4.3-82.6)	6.1	0.80
<i>lnc-ABCB4-1 var1</i>	0.17	0.8 (0.6-1.2)	0.30	6.71e-03	0.7 (0.5-1.0)	0.05	151.4 (67.6-390.8)	492.6 (294.9-955.6)	0.2	5.02e-03
<i>lnc-ABCB4-1 var2</i>	0.54	0.9 (0.6-1.4)	0.70	0.09	0.8 (0.5-1.1)	0.19	230.9 (89.9-427.1)	438.3 (201.4-800.2)	0.3	0.01
<i>lnc-LRIG2-4</i>	0.94	1.2 (1.0-1.5)	0.08	0.77	1.1 (0.9-1.3)	0.33	4.4 (2.3-24.7)	6.9 (2.0-13.8)	1.4	0.93
<i>PVT1</i>	1.23e-03	2.1 (1.4-3.3)	4e-04	8.83e-04	1.7 (1.3-2.2)	3e-04	563.7 (237.3-1295.1)	26.8 (4.6-65.8)	87.3	7e-09
<i>lnc-RAB40AL-2</i>	0.12	1.3 (1.1-1.6)	0.01	0.23	1.3 (1.0-1.5)	0.02	9.2 (4.1-29.6)	6.1 (1.7-18.9)	1.1	0.23
Validation set										
<i>lnc-SERTAD2-3</i>	7.76e-03	1.4 (1.1-1.7)	3.1e-03	4.29e-04	1.6 (1.3-2.0)	2.2e-05	237.7 (86.0-549.8)	14 (1.8-84.3)	8.4	6e-07
<i>lnc-SOX4-1</i>	0.06	1.4 (1.0-1.8)	0.02	0.02	1.7 (1.3-2.2)	2e-04	274.7 (117.9-660.4)	113.01 (39.3-299.6)	3.5	5.29e-03
<i>lnc-HRCT1-1</i>	5.87e-03	1.4 (1.1-1.7)	1.5e-03	5.92e-06	1.5 (1.3-1.9)	2.09e-05	131.2 (66.6-327.7)	10.1 (3.1-50.7)	26.5	2.1e-06
<i>PVT1</i>	1.08e-03	1.3 (1.1-1.6)	4.2e-03	2.67e-07	1.6 (1.3-1.9)	1.24e-05	551.2 (207.8-2375.9)	58.7 (15.2-184.8)	5.5	1e-07

NOTE: RT-qPCR expression levels of selected lncRNA were correlated to OS and PFS in both univariate and multivariate analysis. Data from the training set are reported in the upper part, whilst those for the validation set are reported in the lower part. P values indicate the significance level of the univariate log-rank test; Table summarizes the median distribution (IQR) of fluorescence intensity, normalized, for both relapsers (n = 21 and n = 26 in training and validation set, respectively) and non relapsers (n = 52 and n = 101 in training and validation set, respectively). Ratio is the median distribution of relapsed compared to non relapsers. CI is the confidence interval. In bold are highlighted the lncRNAs found significant in both OS and PFS models. *lnc-ABCB4-1* is reported with two different transcriptional variants (var1 and var2). P^a indicates the level of significance of Cox proportional hazard model. P^b is the level of significance according to the two sides Wilcoxon t test.

**Figure 1.**

Kaplan-Meier curves for lncRNA signature. Figure shows the Kaplan-Meier curves of OS and PFS for *lnc-SERTAD2-3*, *lnc-SOX4-1*, *lnc-HRCT1-1*, and *PVT1* in the cohort of 73 stage I EOC patients of the training set (left, panel A) and on the 129 stage I EOC patients of the validation set (right, panel B). lncRNAs expression levels were converted into discrete variables by dividing the samples into two classes (high, red; low, green), under or over the median. Survival is reported in months (x axis).

lncRNAs is still rudimentary, it is reasonable to assume that the cellular localization of lncRNAs affects their function. Nuclear lncRNAs seem to control transcriptional regulation, whereas cytoplasmic lncRNAs act mainly at the post-transcriptional level. To characterize more accurately the functions of our lncRNAs-based prognostic signature, genome-wide sub-cellular localization studies were performed in five different *in vitro* cellular models of EOC (OVCAR3, OVCAR8, A2780, OVCA432, and CAO3). Abundance of lncRNAs was analyzed in nuclear- and cytoplasmic-enriched fractions. Focusing only on those probes with shared signals across the five cell lines, the analysis identified 513 and 480 lncRNAs probes enriched, respectively, in the nucleus or in cytoplasm (Supplementary Section S3, Supplementary Fig. S3.1 and S3.2, respectively). Robustness of the nuclear and cytoplasmic separation protocols and analyses is supported by confirmation of the nuclear localization of *MALAT1*, *NEAT1*, *TUG1*, and *XLOC_005764*, and the cytoplasmic localization *DANCR/KIAA0114* and *SNHG*, consistent with the literature (24–29).

Expression of *lnc-SOX4-1*, *lnc-SERTAD2-3*, and *PVT1* was higher in the nuclear fraction than in the cytoplasm. *lnc-HRCT1-1* was not differentially localized in the cell lines. It was excluded from downstream experiments. The nuclear enrichment of selected lncRNAs was confirmed in all cell lines by RT-qPCR validation (see Supplementary Fig. S3.3). These results are consistent with the hypothesis that the investigated lncRNAs regulate genome wide transcription regulation, either stabilizing interactions between different proteins or targeting transcription factors to the site of action.

Network analysis: *lnc-SOX4-1*, *lnc-SERTAD2-3*, and *PVT1*

On the basis of the hypothesis that the selected lncRNAs regulate transcription, we generated a co-expression network using matched protein coding genes with expression profiles of lncRNAs and miRNAs (28), to identify genes that are potentially co-regulated with lncRNAs (see Supplementary Section S4). Matched miRNAs expression profiles were extracted from 183 patients previously profiled by our group (ref. 16; Array Express E-MTAB-1067).

Martini et al.

Table 3. Cox model with lncRNAs and histotypes

	Multivariate OS (lncRNA Exp + histotypes)		Multivariate PFS (lncRNA Exp + histotypes)	
	HR (95% CI)	P	HR (95% CI)	P
Clear cell	—	—	—	—
Endometrioid	0.28 (0.1-0.77)	0.013	0.36 (0.14-0.92)	0.032
Mucinous	0.34 (0.12-0.98)	0.045	0.13 (0.03-0.52)	0.003
Serous high grade	0.42 (0.15-1.14)	0.089	0.55 (0.22-1.41)	0.215
Serous low grade	0.15 (0.02-1.18)	0.071	0.44 (0.12-1.71)	0.237
lnc-SOX4-1 Exp	1.57 (1.32-1.85)	1.997e-07	1.62 (1.39-1.88)	4.863e-10
Clear cell	—	—	—	—
Endometrioid	0.34 (0.13-0.94)	0.037	0.41 (0.16-1.06)	0.066
Mucinous	0.5 (0.18-1.41)	0.19	0.19 (0.05-0.73)	0.015
Serous high grade	0.59 (0.22-1.55)	0.284	0.76 (0.31-1.86)	0.543
Serous low grade	0.16 (0.02-1.27)	0.082	0.44 (0.11-1.69)	0.229
lnc-SERTAD2-3 Exp	1.48 (1.26-1.73)	9.357e-07	1.67 (1.43-1.94)	7.654e-11
Clear cell	—	—	—	—
Endometrioid	0.3 (0.11-0.81)	0.017	0.33 (0.13-0.86)	0.023
Mucinous	0.34 (0.12-0.99)	0.046	0.11 (0.03-0.43)	0.0017
Serous high grade	0.49 (0.19-1.31)	0.154	0.63 (0.26-1.55)	0.31
Serous low grade	0.14 (0.02-1.11)	0.062	0.35 (0.09-1.39)	0.135
lnc-HRCT-1 Exp	1.4 (1.24-1.58)	4.418e-08	1.5 (1.35-1.68)	1.625e-13
Clear cell	—	—	—	—
Endometrioid	0.19 (0.06-0.58)	0.0032	0.18 (0.06-0.53)	0.0019
Mucinous	0.48 (0.17-1.34)	0.161	0.18 (0.05-0.7)	0.0131
Serous high grade	0.41 (0.15-1.13)	0.085	0.48 (0.19-1.24)	0.1303
Serous low grade	0.1 (0.01-0.82)	0.031	0.27 (0.07-1.07)	0.062
PVT1 exp	1.43 (1.26-1.62)	1.909e-08	1.54 (1.37-1.74)	1.591e-12

NOTE: The table summarizes multivariate OS and PFS analyses for the four lncRNAs using the histotypes as covariate in the entire cohort of patients. P indicates the level of significance of the Cox proportional hazard model.

For each of the three prognostic lncRNAs, we isolated the most highly correlated genes and computed pathway enrichment. We used the microGraphite pipeline to identify circuits associated with lncRNAs (19). The term circuit refers to a subset of a biological network closely related to lncRNAs expression profile. Circuits associated with the expression of *PVT1* and *lnc-SOX4-1*

were highly interconnected, whereas no circuits could be identified for *lnc-SERTAD2-3*, probably due to the small number of first neighbors identified (see Supplementary Section 4, Supplementary Fig. S4.1 and S4.2).

Figure 2 shows the main genes that in patients with poor prognosis are upregulated and potentially affected by the

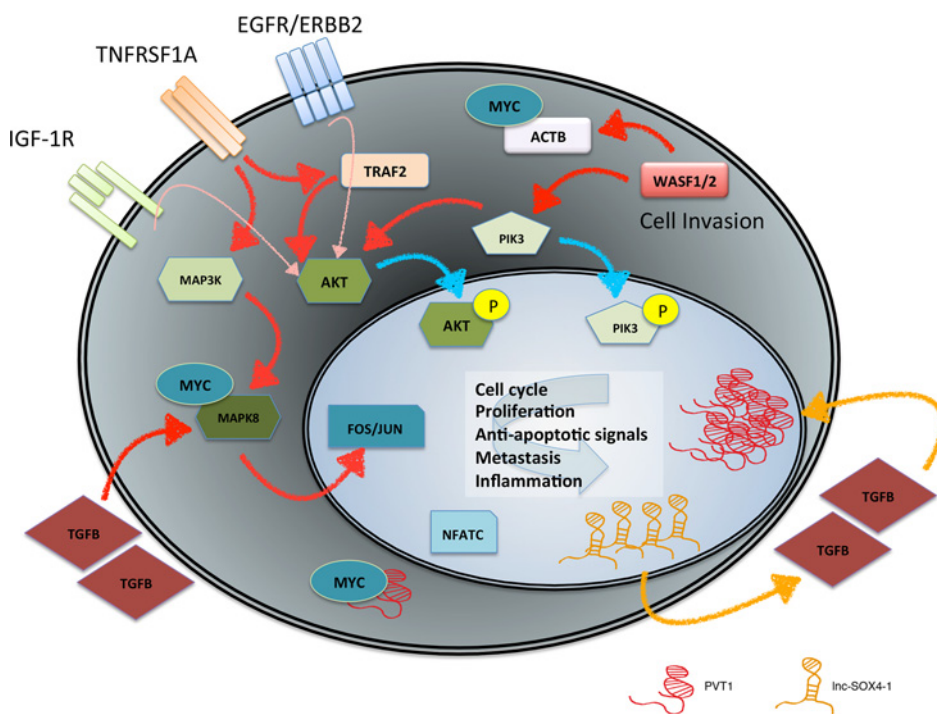


Figure 2. Integrated model of transcriptional-based classifier associated to poor prognosis in stage I EOC. Reconstructed regulatory circuit obtained by the combination of *lnc-SOX4-1* and *PVT1* transcriptional networks associated to poor prognosis. All the genes represented are highly expressed in patients with poor prognosis. *MAPK8* and *ACTB* gene products interact with *MYC* protein according to BioGrid database. The orange arrows have been inferred by data (*lnc-SOX4-1* to *TGFβ*) or derived from literature (*TGFβ* to *PVT1*). Blue arrows represent nuclear translocations and pink arrows represent indirect interactions. Red arrows describe genuine interaction represented in KEGG pathways.

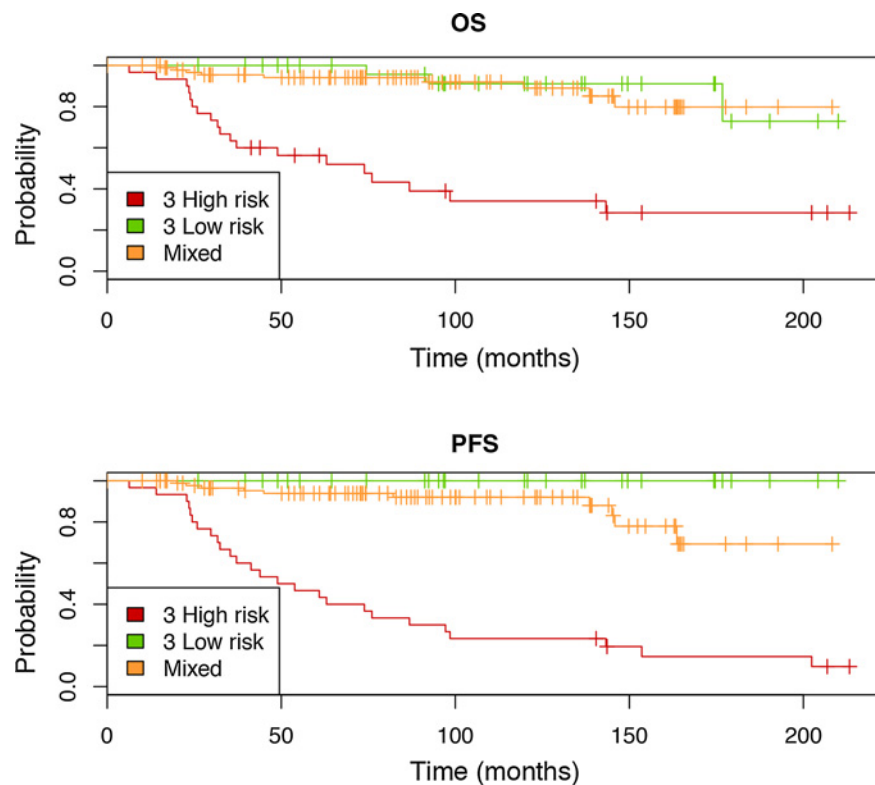


Figure 3.

Kaplan-Meier curves stratifying patients according to *PVT1*, *lnc-SERTAD2-3* and *miR-200c-3p* combined expression. Three classes were built: class "triple high risk" (3 high risk, red) contains patients with both lncRNAs' expression above their median and *miR-200c-3p* below its median; class "triple low risk" (3 low risk, green) contains patients with both lncRNAs' expression below their median and *miR-200c-3p* above the median; class "Mixed" (orange) contains all other patients.

altered expression of *PVT1* and *lnc-SOX4-1* genes. Our data suggest that patients with poor prognosis, that is, those with high levels of *PVT1* or *lnc-SOX4-1*, presented at least two altered signal paths known to be involved in tumor development (29–31). The first one involves *TNFRSF1A*—*TRAF2*—*PIK3/AKT*. The second one starts from *TGF β* and proceeds through *MAPK8/9/10* involving *FOS/JUN*. Both signals sustain processes related to cell cycle, proliferation, antiapoptosis, inflammation and metastasis. These results need to be interpreted in the light of the fact that *WASF1/2* (also known as *WAVE1*) is actively transcribed and co-expressed with *PVT1* in relapsers and in patients with poor prognosis (Fig. 2). *WAVE1* has been reported to induce proliferation by inducing *PIK3/AKT*. The silencing of this gene has been suggested to reduce malignant behavior (32).

Identification of a non-coding signature with prognostic relevance

To evaluate the prognostic performance of the combination of the three selected prognostic lncRNAs, we performed a multivariate survival analysis using both clinical variables (grade, histotypes and chemotherapy treatment regimens) and expression of *PVT1*, *lnc-SOX4-1*, and *lnc-SERTAD2-3*. The model identified as significant the grade (OS, $P = 0.0418$ and PFS $P = 0.00382$), and the expression of *PVT1* (OS $P = 0.0043$ and PFS $P = 0.00372$) and *lnc-SERTAD2-3* (OS $P = 0.0214$ and PFS $P = 0.00045$). The presence of *lnc-SERTAD2-3* rather than *lnc-SOX4-1* in the final model was expected given the strong correlation between *lnc-SERTAD2-3* and *lnc-SOX4-1*. Using a stratification based on *PVT1* and *lnc-SERTAD2-3* expression simultaneously, we achieved better prediction of patients' relapse and survival than when each biomarker was employed alone.

miR-200c-3p was previously identified by our group as a predictor of survival and a biomarker of relapse in stage I EOC (6). Close inspection of the network with the microGraphite pipeline showed that *miR200c-3p* is an element of the *PVT1* circuit (Supplementary Fig. S4.1). To improve further on the definition of an epigenetic non-coding signature with prognostic relevance for stage I EOC, patients' risk of relapse was analyzed using the expression of *miR-200c-3p*, *lnc-SERTAD2-3*, and *PVT1*. *miR-200c-3p* expression values in the entire cohort of patients were newly generated and differences in expression levels between relapsers and non relapsers were confirmed to be significant (see Supplementary Section S2, Supplementary Table S2.5).

We defined a "triple high risk" group of patients on the basis of gene-expression levels in their tumor biopsies, where expression levels of *PVT1* and *lnc-SERTAD2-3* were elevated above their median, whilst levels of *miR-200c-3p* were decreased below its median. Likewise, there was a "triple low-risk" group of patients consisting of those whose tumor biopsies were characterized by expression levels of *PVT1* and *lnc-SERTAD2-3* that were reduced below their median and those of *miR-200c-3p* that were increased above its median. The remaining combinations of risks (2 high and 1 low, 2 low 1 high) were combined into the "mixed-risk" group.

Figure 3 shows KM survival curves of these three groups. Stratification was statistically more significant than that observed when PFS was plotted against any single biomarker (PFS P value = $1e-20$). Using all 202 stage I EOC patients, patients in the "triple high-risk" group had median PFS of 41 months. Patients belonging to the "triple low-risk" group had a median PFS of 131 months (OR, 359.22; 95% CI, 18.47–6986.51). Differences in OS were similar; "triple high-risk" and "triple low-risk" patients presented with median OS values of 36 and 123 months, respectively (OR, 15.55; 95% CI, 3.81–63.36).

Discussion

The results presented in this study pinpoint a prognostic role for transcriptional-based classifiers in the prediction of relapse and outcome of patients with stage I EOC. Two main findings emerge from data. Firstly, the expression levels of the four lncRNAs *lnc-SERTAD2-3*, *lnc-SOX4-1*, *lnc-HRCT1-1*, and *PVT1* are independent prognostic markers of relapse and survival. Second, the combined analysis of the expression profile of *PVT1*, *lnc-SERTAD2-3*, and *miR-200c-3p* can stratify patients' risk of relapse into three discrete classes, high risk, mixed, and low risk. This provides for the first time a non-coding signature with prognostic relevance for stage I EOC.

In the clinical management of stage I EOC, histopathologic-based classifiers, such as FIGO sub-stage and tumor grade, have been hitherto the benchmarks to guide therapeutic decisions. Patients with grade 2 and 3, sub-stage c are routinely treated with adjuvant platinum-based chemotherapy, whilst patients with grade 1, sub-stage a, do not receive any chemotherapy after surgery. It is now recognized that differences within stage I EOC are based on histotype, that is, high- and low-grade serous, endometrioid, mucinous, and clear cells. Each histotype is characterized by different cell morphology, biological behavior and response to therapy (16). Platinum-based therapy is the standard of care shared by these different histologic subtypes. Although the vast majority of stage I EOC patients respond to standard treatment, about 20% of tumors recur and patients ultimately die of resistant disease. The current challenge is to identify those molecular features with prognostic significance that are able to identify at diagnosis those patients at high risk of relapse who would benefit from different treatments, because they benefit little or not at all from standard protocols.

A lot of the research into ovarian cancer focused on the role of protein-coding genes and miRNAs in high-grade serous disease, the most common histotypes (33). This focus neglected the biological and clinical issues associated with stage I EOC, probably because of the rarity of this disease. Less than 10% of EOC are diagnosed as stage I confounding statistical and clinical interpretations. Another reason may be the controversial relationship between stage I and stage III. In contrast with models applied to other solid tumors such as colon cancer, stage I disease is no longer being considered an "early" phase of advanced EOCs. A recent revision of the FIGO classification and results pertaining to the possible pathogenesis of EOC suggest that stage I, especially in the case of non-relapsers, might be a disease completely different from stage III–IV (22).

Previous studies have identified coding and non-coding transcriptional-based classifiers, with prognostic relevance for stage I EOC (5–7). Specifically, *miR-200c-3p* was found to be a biomarker of survival and relapse in stage I EOC being a part of a complex prognostic network consisting of 10 coding genes and 16 miRNAs. This integrated signature classifier (ISC) was used to stratify patients into classes of risk. The ISC performance was better than conventional clinic pathologic-based classifiers in terms of sensitivity and specificity, and it was independent of all clinical and histologic covariates (5).

The present study further corroborates the prognostic importance of epigenetic mechanisms. It is becoming clear that the vast majority of the genome is transcribed into complex families of non-coding RNAs, of which miRNAs are only a small fraction. Non-coding RNAs can be grouped into 2 major classes: short

RNAs, less than 200 bp long (e.g., miRNAs, small nuclear RNAs, PIWI-interacting RNAs), and lncRNAs, ranging from approximately 200 bp to 100 kb. The mammalian genome encodes thousands of lncRNA genes, but only few of them have to date been functionally characterized. Many lncRNAs exert interesting biological functions, including evolutionary conservation (8), disease and tissue-specific expression (13), chromatin remodeling (34), and reprogramming of induced pluripotent stem cells (35). It has also been reported that lncRNAs modulate apoptosis and invasion (34), and reflect cell fate (36). For these reasons lncRNAs are nowadays considered to be major regulatory components of the eukaryotic genome.

Although a detailed biological and functional characterization of the lncRNAs identified here was not the goal of this work, there are some key issues that deserve to be highlighted. *PVT1*, one of the best functionally characterized lncRNAs, is known to act as an oncogene. Consistent with currently known mechanisms of action of *PVT1*, we found that *PVT1* was overexpressed in tumor biopsies of stage I EOC patients with poor prognosis. *PVT1* is located near the *MYC* locus on human chromosome 8q24, and forms a cluster of *MYC*-activating chromosomal translocation breakpoints in different solid and hematologic malignancies (37). Co-amplification of human *MYC* and *PVT1* was reported to correlate with rapid progression of breast cancer and with poor survival of post-menopausal or *HER2*-positive breast cancer patients (38). In multiple myeloma, rearrangements of the *PVT1* region have been shown to correlate with patients' resistance against therapy (39). The recent discovery of a miRNA cluster (*miR-1204*, *miR-1205*, *miR-1206*, *miR-1207*, and *miR-1208*) within the *PVT1* genomic DNA region suggests complex regulation networks within the *MYC-PVT1* locus (40). In our cohort of patients, genomic analysis failed to identify any co-amplification of *PVT1* or *MYC* locus genes, suggesting that increased expression of the *PVT1* gene cannot be due to structural changes in DNA, like copy-number variation (Supplementary Section 5).

Upregulation of *PVT1*, mediated by *TGFβ1*, has been demonstrated to control cellular proliferation and stem cell properties in hepatocellular carcinoma (41). In the *lnc-SOX4-1* circuits, *TGFβ1* is upregulated in patients with poor prognosis. These facts suggest a functional link between *PVT1* and *lnc-SOX4-1* that deserve future investigation. As summarized in Fig. 2, our data suggest that the network engaged by the *PVT1* and *lnc-SOX4-1* circuits share some important genes, like *AKT*, *PIK3* family and the *MAPK* family. As mediators of cell proliferation and cell-cycle progression, they may play a key role in driving tumor relapse in stage I EOC.

It has recently been demonstrated that among the different pathways leading to *AKT/PIK3* activation, *IGF-1R* and *EGFR/ERBB2* are directly involved in platinum resistance of breast and ovarian cancer cell lines (42). Our results are consistent with this notion suggesting that *IGF-1R* and *EGFR/ERBB2* were upregulated in patients with poor prognosis leading to the activation of *AKT/PIK3* and *MAPK*. Moreover, we found the upregulation of *WASF1* (also known as *WAVE1*) a strong promoter of invasiveness and metastasis acting via *AKT/PIK3* and *MAPK* signaling pathways (32).

Relapsing patients presented with upregulated genes that sustained *AKT/PIK3* pathways, where *AKT* is a hub. This finding provides the rationale for the use of *AKT* inhibitors in those patients with a prognostically negative gene signature (29).

Disclosure of Potential Conflicts of Interest

No potential conflicts of interest were disclosed.

Authors' Contributions

Conception and design: R. Fruscio, M. D'Incalci, S. Marchini, C. Romualdi
Development of methodology: P. Martini, E. Calura, G. Sales, C. Romualdi
Acquisition of data (provided animals, acquired and managed patients, provided facilities, etc.): L. Paracchini, M. Mello-Grand, R. Fruscio, A. Ravaggi, E. Bignotti, F.E. Odicino, E. Sartori, D. Katsaros, I. Craparotta, G. Chiorino, L. Ceppi, C. Mangioni, C. Ghimenti
Analysis and interpretation of data (e.g., statistical analysis, biostatistics, computational analysis): P. Martini, R. Fruscio, L. Beltrame, E. Calura, G. Sales, G. Chiorino, L. Mannarino
Writing, review, and/or revision of the manuscript: P. Martini, L. Paracchini, G. Caratti, R. Fruscio, A. Ravaggi, E. Bignotti, F.E. Odicino, E. Sartori, D. Katsaros, M. D'Incalci
Administrative, technical, or material support (i.e., reporting or organizing data, constructing databases): L. Paracchini, L. Beltrame, D. Katsaros
Study supervision: M. D'Incalci, S. Marchini, C. Romualdi
Other (biological experiments and microarray experiments): L. Paracchini
Other (histopathological diagnosis): P. Perego
Other (biological experiments): S. Cagnin

Acknowledgments

We would like to thank Professor Andreas Gescher (Leicester, UK) for critical revision and editing of the manuscript. We are grateful to "Cloud4CARE" project for providing computational resources for data analysis. We thank CRIBI Center for high performance computing resources funded by the Regione Veneto (grant number RISIB project SMUPR no. 4145).

Grant Support

We acknowledge the Nerina and Mario Mattioli Foundation, Alleanza Contro il Tumore Ovarico (ACTO), the Italian Association for Cancer Research (AIRC IG11673 and IG: 15177 to S. Marchini; IG 17185 to C. Romualdi), CARIPLO Foundation (Grant Number x2013-0815 to S. Marchini, C. Romualdi, and E. Sartori; Grant Number 2015-0848 to L. Beltrame and E. Calura), CARIPARO Foundation Project for Excellence 2012 (The Role of coding and non-coding RNA in chronic myeloproliferative neoplasms: from bioinformatics to translational research) to C. Romualdi.

The costs of publication of this article were defrayed in part by the payment of page charges. This article must therefore be hereby marked *advertisement* in accordance with 18 U.S.C. Section 1734 solely to indicate this fact.

Received June 7, 2016; revised October 24, 2016; accepted October 30, 2016; published OnlineFirst November 8, 2016.

References

- Kurman RJ, Shih I-M. The Origin and pathogenesis of epithelial ovarian cancer: a proposed unifying theory. *Am J Surg Pathol* 2010;34:433.
- Sood A, Matsuo K, Gershenson D. Management of early-stage ovarian cancer. In: Bristow RE, Karlan BY, editors. *Surgery for ovarian cancer: principles and practice*. New York, NY: Informa Healthcare; 2010. p. 37–60.
- Vaughan S, Coward JL, Bast RC, Berchuck A, Berek JS, Brenton JD, et al. Rethinking ovarian cancer: recommendations for improving outcomes. *Nat Rev Cancer* 2011;11:719–25.
- Chan JK, Tian C, Teoh D, Monk BJ, Herzog T, Kapp DS, et al. Survival after recurrence in early-stage high-risk epithelial ovarian cancer: a Gynecologic Oncology Group study. *Gynecol Oncol* 2010;116:307–11.
- Calura E, Paracchini L, Fruscio R, Di Feo A, Ravaggi A, Peronne J, et al. A prognostic regulatory pathway in stage I Epithelial Ovarian Cancer: new hints for the poor prognosis assessment. *Ann Oncol* 2016;27:1511–9.
- Marchini S, Cavalieri D, Fruscio R, Calura E, Garavaglia D, Nerini IF, et al. Association between miR-200c and the survival of patients with stage I epithelial ovarian cancer: a retrospective study of two independent tumour tissue collections. *Lancet Oncol* 2011;12:273–85.
- Marchini S, Mariani P, Chiorino G, Marrazzo E, Bonomi R, Fruscio R, et al. Analysis of gene expression in early-stage ovarian cancer. *Clin Cancer Res* 2008;14:7850–60.
- Guttman M, Amit I, Garber M, French C, Lin MF, Feldser D, et al. Chromatin signature reveals over a thousand highly conserved large non-coding RNAs in mammals. *Nature* 2009;458:223–7.
- Hu W, Alvarez-Dominguez JR, Lodish HF. Regulation of mammalian cell differentiation by long non-coding RNAs. *EMBO Rep* 2012;13:971–83.
- Mercer TR, Dinger ME, Mattick JS. Long non-coding RNAs: insights into functions. *Nat Rev Genet* 2009;10:155–9.
- Ponting CP, Oliver PL, Reik W. Evolution and functions of long noncoding RNAs. *Cell* 2009;136:629–41.
- Rinn JL, Chang HY. Genome regulation by long noncoding RNAs. *Annu Rev Biochem* 2012;81:145–66.
- Mattick JS. The genetic signatures of noncoding RNAs. *PLoS Genet* 2009;5:e1000459.
- Huarte M, Rinn JL. Large non-coding RNAs: missing links in cancer? *Hum Mol Genet* 2010;19:R152–61.
- Iyer MK, Niknafs YS, Malik R, Singhal U, Sahu A, Hosono Y, et al. The landscape of long noncoding RNAs in the human transcriptome. *Nat Genet* 2015;47:199–208.
- Calura E, Fruscio R, Paracchini L, Bignotti E, Ravaggi A, Martini P, et al. miRNA landscape in stage I epithelial ovarian cancer defines the histotype specificities. *Clin Cancer Res* 2013;19:4114–23.
- McShane LM, Altman DG, Sauerbrei W, Taube SE, Gion M, Clark GM. Reporting recommendations for tumour MARKer prognostic studies (REMARK). *Br J Cancer* 2005;93:387–91.
- Sales G, Romualdi C. parmigene—a parallel R package for mutual information estimation and gene network reconstruction. *Bioinformatics* 2011;27:1876–7.
- Calura E, Martini P, Sales G, Beltrame L, Chiorino G, D'Incalci M, et al. Wiring miRNAs to pathways: a topological approach to integrate miRNA and mRNA expression profiles. *Nucleic Acids Res* 2014;42:e96.
- Sales G, Calura E, Cavalieri D, Romualdi C. graphite-a Bioconductor package to convert pathway topology to gene network. *BMC Bioinformatics* 2012;13:20.
- Martini P, Sales G, Massa MS, Chiogna M, Romualdi C. Along signal paths: an empirical gene set approach exploiting pathway topology. *Nucleic Acids Res* 2013;41:e19.
- Prat J, FIGO Committee on Gynecologic Oncology. Staging classification for cancer of the ovary, fallopian tube, and peritoneum. *Int J Gynecol Obstet* 2014;124:1–5.
- Cannistra SA. Cancer of the ovary. *N Engl J Med* 2004;351:2519–29.
- Bernard D, Prasanth KV, Tripathi V, Colasse S, Nakamura T, Xuan Z, et al. A long nuclear-retained non-coding RNA regulates synaptogenesis by modulating gene expression. *EMBO J* 2010;29:3082–93.
- Cabili MN, Dunagin MC, McClanahan PD, Biaesch A, Padovan-Merhar O, Regev A, et al. Localization and abundance analysis of human lncRNAs at single-cell and single-molecule resolution. *Genome Biol* 2015;16:20.
- Clemson CM, Hutchinson JN, Sara SA, Ensminger AW, Fox AH, Chess A, et al. An architectural role for a nuclear noncoding RNA: NEAT1 RNA is essential for the structure of paraspeckles. *Mol Cell* 2009;33:717–26.
- van Heesch S, van Iterson M, Jacobi J, Boymans S, Essers PB, de Bruijn E, et al. Extensive localization of long noncoding RNAs to the cytosol and mono- and polyribosomal complexes. *Genome Biol* 2014;15:R6.
- Margolin AA, Nemenman I, Basso K, Wiggins C, Stolovitzky G, Favera RD, et al. ARACNE: an algorithm for the reconstruction of gene regulatory networks in a mammalian cellular context. *BMC Bioinformatics* 2006;7:S7.
- LoPiccolo J, Blumenthal GM, Bernstein WB, Dennis PA. Targeting the PI3K/Akt/mTOR pathway: effective combinations and clinical considerations. *Drug Resist Updat* 2008;11:32–50.
- Hers I, Vincent EE, Tavaré JM. Akt signalling in health and disease. *Cell Signal* 2011;23:1515–27.
- Martelli AM, Tabellini G, Bressanin D, Ognibene A, Goto K, Cocco L, et al. The emerging multiple roles of nuclear Akt. *Biochim Biophys Acta* 2012;1823:2168–78.

Martini et al.

32. Zhang J, Zhou S, Tang L, Shen L, Xiao L, Duan Z, et al. WAVE1 gene silencing via RNA interference reduces ovarian cancer cell invasion, migration and proliferation. *Gynecol Oncol* 2013;130:354–61.
33. Weinstein JN, Collisson EA, Mills GB, Shaw KRM, Ozenberger BA, Ellrott K, et al. The cancer genome atlas pan-cancer analysis project. *Nat Genet* 2013;45:1113–20.
34. Khalil AM, Guttman M, Huarte M, Garber M, Raj A, Morales DR, et al. Many human large intergenic noncoding RNAs associate with chromatin-modifying complexes and affect gene expression. *Proc Natl Acad Sci U S A* 2009;106:11667–72.
35. Loewer S, Cabili MN, Guttman M, Loh Y-H, Thomas K, Park IH, et al. Large intergenic non-coding RNA-RoR modulates reprogramming of human induced pluripotent stem cells. *Nat Genet* 2010;42:1113–7.
36. Ginger MR, Shore AN, Contreras A, Rijnkels M, Miller J, Gonzalez-Rimbau MF, et al. A noncoding RNA is a potential marker of cell fate during mammary gland development. *Proc Natl Acad Sci* 2006;103:5781–6.
37. Shtivelman E, Bishop JM. The PVT gene frequently amplifies with MYC in tumor cells. *Mol Cell Biol* 1989;9:1148–54.
38. Borg A, Baldetorp B, Fernö M, Olsson H, Sigurdsson H. c-myc amplification is an independent prognostic factor in postmenopausal breast cancer. *Int J Cancer* 1992;51:687–91.
39. Palumbo AP, Boccadoro M, Battaglio S, Corradini P, Tschlis PN, Huebner K, et al. Human homologue of Moloney leukemia virus integration-4 locus (MLVI-4), located 20 kilobases 3' of the myc gene, is rearranged in multiple myelomas. *Cancer Res* 1990;50:6478–82.
40. Huppi K, Volfovsky N, Runfola T, Jones TL, Mackiewicz M, Martin SE, et al. The identification of microRNAs in a genomically unstable region of human chromosome 8q24. *Mol Cancer Res* 2008;6:212–21.
41. Wang F, Yuan J-H, Wang S-B, Yang F, Yuan S-X, Ye C, et al. Oncofetal long noncoding RNA PVT1 promotes proliferation and stem cell-like property of hepatocellular carcinoma cells by stabilizing NOP2. *Hepatology* 2014;60:1278–90.
42. Eckstein N. Platinum resistance in breast and ovarian cancer cell lines. *J Exp Clin Cancer Res* 2011;30:91.

Clinical Cancer Research

lncRNAs as Novel Indicators of Patients' Prognosis in Stage I Epithelial Ovarian Cancer: A Retrospective and Multicentric Study

Paolo Martini, Lara Paracchini, Giulia Caratti, et al.

Clin Cancer Res 2017;23:2356-2366. Published OnlineFirst November 8, 2016.

Updated version Access the most recent version of this article at:
doi:[10.1158/1078-0432.CCR-16-1402](https://doi.org/10.1158/1078-0432.CCR-16-1402)

Supplementary Material Access the most recent supplemental material at:
<http://clincancerres.aacrjournals.org/content/suppl/2016/12/30/1078-0432.CCR-16-1402.DC2>

Cited articles This article cites 41 articles, 9 of which you can access for free at:
<http://clincancerres.aacrjournals.org/content/23/9/2356.full#ref-list-1>

E-mail alerts [Sign up to receive free email-alerts](#) related to this article or journal.

Reprints and Subscriptions To order reprints of this article or to subscribe to the journal, contact the AACR Publications Department at pubs@aacr.org.

Permissions To request permission to re-use all or part of this article, use this link
<http://clincancerres.aacrjournals.org/content/23/9/2356>.
Click on "Request Permissions" which will take you to the Copyright Clearance Center's (CCC) Rightslink site.